Applied and Computational Mechanics 19 (2025) 105–124

Applied and Computational Mechanics

Free vibration analysis of nanoscale spinning shafts based on Eringen's differential constitutive elastic model by using generalized differential quadrature method

A. Belhadj[a,*], A. Boukhalfa[a], S. A. Belalia[a]

[a] *Computational Mechanics Laboratory (MECACOMP), Department of Mechanical Engineering, Faculty of Technology, University of Tlemcen, Chetoune, BP230, Tlemcen, Algeria*

Received 17 April 2025; accepted 2 October 2025

Abstract

The free vibration behavior of spinning nanoshafts is critically examined through the framework of nonlocal elasticity. Combining the Euler-Bernoulli beam model with the Eringen's nonlocal theory, this work formulates a scale-dependent mathematical model. Hamilton's principle is employed to derive the nonlocal governing equations and associated boundary conditions. The generalized differential quadrature method (GDQM) is utilized to discretize and solve the resulting eigenvalue problem. Numerical results systematically quantify how the small-scale parameter, angular velocity, and various boundary conditions affect the system's fundamental and second mode forward and backward frequencies. Additionally, the impact of geometrical properties, such as the aspect ratio and thickness-to-diameter ratio, on the instability thresholds is investigated. The findings of this study offer valuable guidelines for enhancing the performance and stability of advanced rotating nano-electromechanical systems (NEMS).

Keywords: vibration, spinning shafts, nanoscale, nonlocal elasticity, GDQM

1. Introduction

Rotating machinery has attracted considerable research and development interest, particularly in the areas of monitoring, diagnostics, theoretical modeling, and dynamic analysis [6, 13, 23, 27, 30, 50]. Driven by the scientific and technological revolution at the end of the 20th century, contemporary research and engineering have undergone transformative developments. The paradigm of miniaturization has profoundly transformed the industrial landscape, establishing a dynamic field of research dedicated to advanced nanotechnological applications. These range from small-scale motors and robotic actuators to fully functional computers smaller than a biological cell. The realization of such nano-electromechanical systems (NEMS) [19] relies critically on the performance of constituent nanostructures, including nanobeams, nanowires, and nanoplates. Although the mechanical properties of these elements can be studied using molecular dynamics (MD) simulations [22], the significant computational expense associated with this method often renders it impractical. Therefore, continuum-based theoretical frameworks are widely employed as a computationally efficient alternative for mechanical analysis at the nanoscale [9].

Eringen's nonlocal continuum theory [15,16] offers a particularly useful framework. In contrast to classical elasticity, it considers the stress at a point to be a function of strains throughout

*Corresponding author. Tel.: +213 661 823 466, e-mail: belhabdelkadir@gmail.com.
https://doi.org/10.24132/acm.2025.999

the entire body, leading to more reliable results for small-scale structures. Eringen [17] also established a formal relationship between nonlocal elasticity and lattice dynamics, showing that their equations of motion and potential energy expressions are consistent. Today, nonlocal elasticity models are widely used to analyze size-dependent mechanical behavior in nanostructures [1, 11]. The discovery of carbon nanotube [28] has been a determinant and a big step for the world of technology; their exceptional mechanical and electrical properties have opened up new perspectives for their application in various fields such as medicine, defense, NEMS and material sciences. Nanostructures undergoing rotation are systems with a promising future to be used in nanomachines which include nanomotors devices such as fullerene gears and carbon nanotube gears [20] and bearings [7, 46]. The understanding of nanosturctures mechanical behavior such as bending, buckling and vibration is required to develop an efficient design of these small-scale devices where the nonlocal effect becomes prominent. Previous studies have extensively employed nonlocal elasticity to investigate the vibration of nanostructures [10, 49]. For example, Murmu and Adhikari [34] examined the effect of nonlocality on the bending-vibration of a pre-stressed single-walled carbon nanotube, noting the influence of preload, angular velocity, and nonlocal parameter. In [52], Thai developed a nonlocal shear deformation beam theory for the bending, buckling, and vibration of nanobeams, deriving analytical solutions for simply supported beams that aligned closely with Timoshenko and Reddy beam theories [40]. Eltaher et al. [18] introduced a finite element model for nonlocal Euler-Bernoulli beams and studied the effects of the nonlocal parameter, slenderness ratio, rotary inertia, and boundary conditions. More recent work has applied the differential quadrature method (DQM) to analyze rotating cantilever nanobeams made of isotropic [26, 33, 35, 39, 47] and functionally graded materials [2, 14, 37, 45], including studies considering various surrounding media and stress conditions.

It is noted that the use of nonlocal elasticity theory suffers from a misunderstanding of the key concept of nonlocality [44], which has led to some recent erroneous scientific results due to the use of nonlocal strain gradient theory, which proposed a combination of the nonlocal theory with the strain gradient theory. It was believed that the strain gradient theory could only capture the hardening behavior of the material while the nonlocal theory could only capture the softening. However, in reality, both theories can give both the hardening and softening behavior of the material. Moreover, the strain gradient theory is a nonlocal theory with finite neighbor interactions. So combining it with the nonlocal model into a single unified formulation is not physically meaningful. Fernández-Sáez et al. [21] proposed an integral constitutive equation to formulate the static bending of Euler-Bernoulli beam with different boundary conditions, they remarked the appearance of a paradox when solving the cantilever beam with the differential form of the Eringen model (increase in stiffness with the nonlocal parameter) and they solved it. In [42, 43], Sae-Long et al. have studied a rational beam-elastic substrate model with inclusion of nonlocal and surface-energy effects to demonstrate the capability of the proposed model in eliminating the paradoxical behavior present in the Eringen nonlocal differential model. They have employed a fourth-order strain gradient model based on a thermodynamic approach to analyze isotropic and homogeneous nanowire embedded in an elastic substrate.

Applying the Eringen size-dependent model in its differential form requires that the physically admissible boundary conditions shall be consistent with the underlying kernel of the differential model and are explicitly derived and applied. This correctly predicts the qualitative trend of "stiffness-softening" and has been successfully used in countless studies to model size-effects, providing results that are often consistent with experimental data and molecular dynamics simulations for many problems [24, 25, 36].

Recently in [4], we studied the free vibration behavior of a rotating nanoshaft in the form of a single-walled carbon nanotube (SWCNT). The results showed that the use of SWCNT in rotating nano-machinery can be a good choice due to exceptional mechanical properties that offer carbon nanotubes (CNTs). The nanoshaft structure was studied with and without rotation, whereas the flexural bending vibration results have been compared and found in agreement with the results by Chakraverty and Behera [8].

While the free vibration of stationary nano-beams has been extensively studied, the analysis of spinning nano-structures remains relatively unexplored. The current study bridges this gap by presenting a comprehensive nonlocal elasticity analysis of the free vibration of spinning nanoshafts. The novel aspects of this work are threefold: First, it uniquely investigates the coupled effect of the small-scale parameter and the gyroscopic forces induced by spinning on both the forward and backward whirling frequencies, a phenomenon scarcely addressed in existing literature. Second, it introduces a robust solution framework by applying the generalized differential quadrature method (GDQM) to the derived nonlocal equations, demonstrating its efficacy in handling the complex boundary value problems inherent to spinning systems. Third, it provides new physical insights by systematically quantifying how angular velocity and boundary conditions dictate the instability thresholds and frequency splitting in nanoshafts, revealing that the small-scale effect significantly alters critical speeds compared to the classical local theory. In this work, Campbell diagrams have been involved to identify critical speed parameters for different nonlocal parameters. Then, a parametric study has been done to investigate different geometrical properties for different boundary conditions. The findings, which include novel data on the influence of the aspect ratio and thickness-to-diameter ratio, offer indispensable design guidelines for the development of high-performance, stable rotating nano-machinery and NEMS.

2. Mathematical modelling

Unlike the classical theory of elasticity, the theory of nonlocal elasticity assumes that the stress depends not only on the strain at a certain point but also on strains at all other points of the body. The nonlocal theory considers long-range inter-atomic interaction and yields results dependent on the size of a body. In the following text, the simplified form of the Eringen's nonlocal constitutive equation is applied to a Hookean solid as [10]

$$\left[1 - (e_0\, a)^2\, \nabla^2\right] \sigma_{nl} = \sigma_l, \tag{1}$$

where ∇^2 is the Laplacian operator, $(e_0\, a)^2$ is a nonlocal parameter, σ_{nl} is the nonlocal stress, and σ_l stands for the local stress.

Let us consider a nanobeam of length L and radius r, rotating around its longitudinal axis with a constant rotational speed, Fig. 1. Previous investigations showed that the Euler-Bernoulli beam theory (EBT) offers a reliable model for one-dimensional nanostructures such as CNTs. The cross-section remains planar during the flexure and the beam deflection is small. The rotating nanoshaft geometry is referred to the Cartesian coordinate system and modelled based on EBT as follows [4]:

$$\begin{aligned} u_x(x,y,z,t) &= u(x,t) - z\frac{\partial v(x,t)}{\partial x} - y\frac{\partial w(x,t)}{\partial x}, \\ u_y(x,y,z,t) &= v(x,t), \\ u_z(x,y,z,t) &= w(x,t), \end{aligned} \tag{2}$$

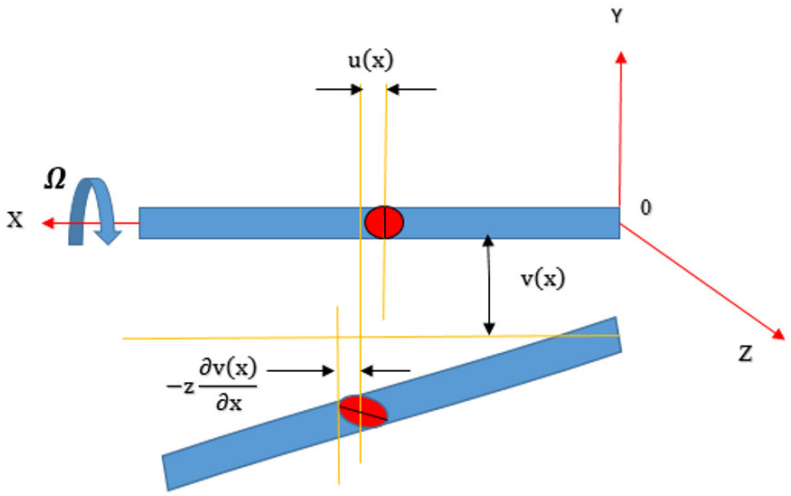

Fig. 1. Geometry of the nanoshaft during rotation

where u_x, u_y and u_z, are the axial, lateral and transverse displacements, respectively, $\frac{\partial v(x,t)}{\partial x}$ and $\frac{\partial w(x,t)}{\partial x}$ denote the rotation of the cross-section about the y- and z-axes, respectively. The local strain has the following form:

$$\varepsilon_{xx} = \frac{\partial u}{\partial x} - z\frac{\partial^2 v}{\partial x^2} - y\frac{\partial^2 w}{\partial x^2}. \tag{3}$$

Then, the local stress-strain relationship shall be defined as

$$\sigma_{xx} = E\,\varepsilon_{xx} = E\left(\frac{\partial u}{\partial x} - z\frac{\partial^2 v}{\partial x^2} - y\frac{\partial^2 w}{\partial x^2}\right), \tag{4}$$

where E is the Young's modulus.

Based on the Hamilton's principle, the motion of an elastic structure over a time interval is reduced to zero by combining the virtual displacements and virtual forces [46], i.e.,

$$\int_{t_1}^{t_2} (\delta U + \delta V - \delta K)\,\mathrm{d}t = 0, \tag{5}$$

where δU, δV, δK are the variations of the strain energy, potential energy and kinetic energy, respectively, and t_1 and t_2 represent the initial and final times. The strain energy is expressed as [4]

$$U = \frac{1}{2}\int_0^L \int_A (\sigma_{xx}\,\delta\varepsilon_{xx})\,\mathrm{d}A\,\mathrm{d}x, \tag{6}$$

For the kinetic energy, we have [4]

$$K = \frac{1}{2}\int_0^L \left\{ \varrho A\left[\left(\frac{\partial u}{\partial t}\right)^2 + \left(\frac{\partial v}{\partial t}\right)^2 + \left(\frac{\partial w}{\partial t}\right)^2\right] + \varrho I 2\Omega\left[\left(\frac{\partial^2 v}{\partial t\partial x}\right)^2 + \left(\frac{\partial^2 w}{\partial t\partial x}\right)^2\right]\left(\frac{\partial^2 v}{\partial t\partial x}\frac{\partial w}{\partial t} - \frac{\partial^2 w}{\partial t\partial x}\frac{\partial v}{\partial t}\right) + 2\Omega^2\right\}\mathrm{d}x, \tag{7}$$

where ϱ is the mass density, A is the cross-section, I is the moment of inertia of the cross-section, and Ω is the angular velocity of the rotating nanoshaft.

Substituting (6) and the variation of (7) into (5) and integrating by parts then collecting the coefficients δu, δv, δw yield the following equations of motion:

$$\begin{aligned}
\delta u: &\quad \varrho A\frac{\partial u^2}{\partial t^2} = \frac{dN}{dx},\\
\delta v: &\quad \varrho A_y\frac{\partial v^2}{\partial t^2} + \varrho I\frac{\partial v}{\partial t} - 2\Omega\left(\frac{\partial w}{\partial t}\right) = \frac{\partial^2 M_y}{\partial^2 x},\\
\delta w: &\quad \varrho A_z\frac{\partial w^2}{\partial t^2} + \varrho I\frac{\partial w}{\partial t} + 2\Omega\left(\frac{\partial v}{\partial t}\right) = \frac{\partial^2 M_z}{\partial^2 x},
\end{aligned} \tag{8}$$

where $I = I_y = I_z$ are the moment of inertia relative to x, y, and z axis, and A, A_y, A_z are defined as follows:

$$(A, A_y, A_z) = \int_A (1, z, y)\,\mathrm{d}A. \tag{9}$$

By applying the nonlocal elasticity theory formulated in (1) to the resultant stress in the direction of x-, y-, and z-axes, we obtain the following system of equations:

$$\begin{aligned}
\varrho A\left[\ddot{u} - (e_0\,a)^2\frac{d^2\ddot{u}}{dx^2}\right] &= EA\frac{d^2u}{dx^2},\\
\varrho A_y\left[\ddot{v} - (e_0\,a)^2\frac{d^2\ddot{v}}{dx^2}\right] + \varrho I\left[\dot{v} - (e_0\,a)^2\frac{d^2\dot{v}}{dx^2}\right] - 2\Omega\left(\dot{w} - (e_0\,a)^2\frac{d^2\dot{w}}{dx^2}\right) &= EI\frac{d^4v}{dx^4},\\
\varrho A_z\left[\ddot{w} - (e_0\,a)^2\frac{d^2\ddot{w}}{dx^2}\right] + \varrho I\left[\dot{w} - (e_0\,a)^2\frac{d^2\dot{w}}{dx^2}\right] + 2\Omega\left(\dot{v} - (e_0\,a)^2\frac{d^2\dot{v}}{dx^2}\right) &= EI\frac{d^4w}{dx^4}.
\end{aligned} \tag{10}$$

3. Generalized differential quadrature method (GDQM)

Differential quadrature method (DQM) has been successfully used to solve both linear and nonlinear multiscale structural problems efficiently and accurately. It was introduced for the first time by Bellman et al. in 1972 [3], because it provides simple formulation and low computational cost. It has been widely used for solving different problems in computational mechanics [5]. The main idea of DQM is to quickly compute the derivative of a function at any grid point within its bounded domain by estimating a weighted linear sum of values of the function at a small set of points related to the domain.

In order to show the mathematical formulation of DQM, let $f(x)$ be a continuous function on the interval $[a, b]$. Then the n-th order derivative of the function $f(x)$ at an intermediate point (grid point) x_i can be written as follows:

$$\left|\frac{d^n f}{dx^n}\right|_{x=x_i} = \sum_{j=1}^{N} {C_{ij}}^{(n)} f\left(x_j\right), \quad i = 1, 2, \ldots, N,\ n = 1, 2, \ldots, N-1, \tag{11}$$

where ${C_{ij}}^{(n)}$ is the weighting coefficient of the n-th order derivative, and N the number of grid points of the whole domain ($a = x_1, x_2, \ldots, x_i, \ldots, x_N = b$).

According to Lo et al. [31] who have proposed the generalized differential quadrature method (GDQM) for solving partial differential equations in fluid mechanics, the weighting

coefficients of the first-order derivatives in the direction of $\xi = \frac{x}{L}$ are determined as [48]

$$C_{i,j}^{(1)} = \frac{P(\xi_i)}{(\xi_i - \xi_j) P(\xi_j)},\ i,j = 1,2\ldots,N,\ i \neq j, \qquad C_{i,i}^{(1)} = -\sum_{\substack{j=1 \\ j\neq i}}^{N} C_{i,j}^{(1)}, \tag{12}$$

where

$$P(\xi_i) = \prod_{j=1}^{N} (\xi_i - \xi_j),\ i \neq j. \tag{13}$$

Then, the second- and higher-order derivatives are calculated

$$C_{i,j}^{(2)} = \sum_{k=1}^{N} C_{i,k}^{(1)} C_{k,j}^{(1)},\ i = j = 1,2\ldots,N, \tag{14}$$

$$C_{i,j}^{(r)} = \sum_{k=1}^{N} C_{i,k}^{(1)} C_{k,j}^{(r-1)},\ i = j = 1,2\ldots,N,\ r = 2,3\ldots,m\ (m < N). \tag{15}$$

In structural dynamics, many studies have been elaborated using GDQM [12, 32] that help us to understand the numerical method and exploit it for our nonlocal size-dependent eigen-problem. Throughout the paper, the grid points are considered based on the well-established Chebyshev-Gauss-Lobatto points

$$\xi_i = \frac{1}{2}\left[1 - \frac{\cos(i-1)\pi}{N-1}\right],\ i = 1,2\ldots,N. \tag{16}$$

4. Discrete governing equations and boundary conditions

The longitudinal, lateral and transverse deflection are respectively defined as follows:

$$u(x,t) = ue^{i\omega t}, \quad v(x,t) = ve^{i\omega t}, \quad w(x,t) = we^{i\omega t}.$$

For convenience and generality, the following non-dimensional variables are introduced as: element location ξ, nonlocal parameter μ, hub-radius δ, frequency parameter λ, angular velocity parameter γ, moment of inertia parameter Γ and the non-dimensional deflections U, V, and W

$$\xi = \frac{x}{L}, \quad \mu = \frac{e_0\, a}{L}, \quad \delta = \frac{r}{L}, \quad \lambda^2 = \frac{\varrho A L^4 \omega^2}{EI}, \quad \gamma^2 = \frac{\varrho A L^4 \Omega^2}{EI},$$
$$\Gamma = \frac{I}{AL}, \quad U = \frac{u}{x}, \quad V = \frac{v}{x}, \quad W = \frac{w}{x}.$$

Assuming $A_{i,j}$, $B_{i,j}$, $C_{i,j}$, $D_{i,j}$ are respectively the first, second, third, and fourth derivatives, the discretization of the governing nonlocal non-dimensional equations using DQM gives the following system of equations:

$$-\frac{\lambda^2}{L^2}\left(1 - \mu^2 \sum_{j=1}^{N} B_{i,j}\right) U_j - EA \sum_{j=1}^{N} B_{i,j} U_j = 0, \tag{17}$$

$$-\lambda^2\left(1-\mu^2\sum_{j=1}^{N}B_{i,j}\right)V_j+\Gamma\lambda j\left(1-\mu^2\sum_{j=1}^{N}B_{i,j}\right)V_j - \frac{2\gamma^2}{\varrho\pi\delta^2L^2}j\left(1-\mu^2\sum_{j=1}^{N}B_{i,j}\right)W_j-\sum_{j=1}^{N}D_{i,j}V_j=0, \tag{18}$$

$$-\lambda^2\left(1-\mu^2\sum_{j=1}^{N}B_{i,j}\right)W_j+\Gamma\lambda j\left(1-\mu^2\sum_{j=1}^{N}B_{i,j}\right)W_j + \frac{2\gamma^2}{\varrho\pi\delta^2L^2}j\left(1-\mu^2\sum_{j=1}^{N}B_{i,j}\right)V_j-\sum_{j=1}^{N}D_{i,j}W_j=0. \tag{19}$$

The big challenge of using GDQM for this kind of problems is the boundary conditions imposition, which are incorporated by modifying the weighting coefficients. All the elements in the columns corresponding to the points of boundary conditions in the weighting coefficients matrix are set to zero [29, 51]. In the present work, the boundary conditions used for the free vibration of rotating nonlocal shaft are formulated as follows:

As we are interested in the flexural vibration behavior of nano-rotors, this study takes into consideration only the two equations of flexion. So, we define [29]

$$V_i^{(1)}=\sum_{j=1}^{N}A_{ij}\,V_j,\quad V_i^{(2)}=\sum_{j=1}^{N}B_{ij}\,V_j,\quad V_i^{(3)}=\sum_{j=1}^{N}C_{ij}\,V_j,\quad V_i^{(4)}=\sum_{j=1}^{N}D_{ij}\,V_j. \tag{20}$$

The weighting coefficients A_{ij} and the modified weighting coefficients that are a combination of two matrices $[\bar{A}_1]$ and $[\bar{A}_2]$ are

$$\begin{bmatrix}A_{11}&A_{12}&\dots&A_{1N-1}&A_{1N}\\ \vdots&\vdots&\dots&\vdots&\vdots\\ A_{N1}&A_{N2}&\dots&A_{NN-1}&A_{NN}\end{bmatrix}\begin{Bmatrix}V_1\\ \vdots\\ V_N\end{Bmatrix}=\begin{Bmatrix}{V_1}^{(1)}\\ \vdots\\ {V_N}^{(1)}\end{Bmatrix}, \tag{21}$$

$$[\bar{A}_1]=\begin{bmatrix}0&A_{12}&\dots&A_{1N-1}&A_{1N}\\ \vdots&\vdots&\dots&\vdots&\vdots\\ 0&A_{N2}&\dots&A_{NN-1}&A_{NN}\end{bmatrix},\quad [\bar{A}_2]=\begin{bmatrix}A_{11}&A_{12}&\dots&A_{1N-1}&0\\ \vdots&\vdots&\dots&\vdots&\vdots\\ A_{N1}&A_{N2}&\dots&A_{NN-1}&0\end{bmatrix}. \tag{22}$$

As Fernández-Sáez et al. [21] have already shown that only for cantilever beam, the differential form of the Eringen nonlocal model gives inconsistent results compared to those of its integral form. Considering also that a rotating shaft could not be in a cantilever condition, three boundary conditions (BCs) shall be imposed: a simply supported (S-S) beam, a simply supported clamped (S-C) beam and a bi-clamped (C-C) beam. These boundary conditions shall be consistent with the underlying kernel of the differential model that shall be also equivalent to the integral form. This equivalence is guaranteed if the nonlocality boundary conditions are concomitantly satisfied [38].

We define herein below the employed BCs: For the S-S beam, $V_1=V_N=0$:

$$\begin{bmatrix}0&A_{12}&\dots&A_{1N-1}&0\\ \vdots&\vdots&\dots&\vdots&\vdots\\ 0&A_{N2}&\dots&A_{NN-1}&0\end{bmatrix}\begin{Bmatrix}V_1\\ \vdots\\ V_N\end{Bmatrix}=\begin{Bmatrix}{V_1}^{(1)}\\ \vdots\\ {V_N}^{(1)}\end{Bmatrix}. \tag{23}$$

The first derivative is expressed as

$$\left\{V^{(1)}\right\} = \left[\bar{A}\right]\{V\}, \qquad \left\{V^{(2)}\right\} = [A]\left\{V^{(1)}\right\}, \tag{24}$$

Using $(24)_2$, the second derivative can be written as

$$\left\{V^{(2)}\right\} = [A]\left[\bar{A}\right]\{V\} = \left[\bar{B}\right]\{V\}. \tag{25}$$

As ${V_1}^{(3)} = {V_N}^{(3)} = 0$, the third derivative is computed as

$$\left\{V^{(3)}\right\} = \left[\bar{A}\right]\left\{V^{(2)}\right\} = \left[\bar{A}\right]\left[\bar{B}\right]\{V\} = \left[\bar{C}\right]\{V\}. \tag{26}$$

Then, the fourth derivative has the form

$$\left\{V^{(4)}\right\} = \left[\bar{A}\right]\left\{V^{(3)}\right\} = \left[\bar{A}\right]\left[\bar{B}\right]\left[\bar{C}\right]\{V\} = \left[\bar{D}\right]\{V\}. \tag{27}$$

Following the same formulation, the clamped-clamped boundary condition yields

$$\begin{aligned}
&\left\{V^{(1)}\right\} = \left[\bar{A}\right]\{V\},\\
&\left\{V^{(2)}\right\} = \left[\bar{A}\right]\left\{V^{(1)}\right\} = \left[\bar{B}\right]\{V\}, \quad \left[\bar{B}\right] = \left[\bar{A}\right]\left[\bar{A}\right],\\
&\left\{V^{(3)}\right\} = [A]\left\{V^{(2)}\right\} = [A]\left[\bar{B}\right]\{V\} = \left[\bar{C}\right]\{V\}, \quad \left[\bar{C}\right] = \left[\bar{A}\right]\left[\bar{B}\right],\\
&\left\{V^{(4)}\right\} = [A]\left\{V^{(3)}\right\} = [A]\left[\bar{C}\right]\{V\} = \left[\bar{D}\right]\{V\}, \quad \left[\bar{D}\right] = [A]\left[\bar{C}\right].
\end{aligned} \tag{28}$$

For the S-C beam, we get

$$\begin{aligned}
&\left\{V^{(1)}\right\} = \left[\bar{A}\right]\{V\},\\
&\left\{V^{(2)}\right\} = \left[\bar{A}_2\right]\left\{V^{(1)}\right\} = \left[\bar{A}_2\right]\left[\bar{A}\right]\{V\} = [\bar{B}]\{V\}, \quad \left[\bar{B}\right] = \left[\bar{A}_2\right]\left[\bar{A}\right],\\
&\left\{V^{(3)}\right\} = \left[\bar{A}_1\right]\left\{V^{(2)}\right\} = \left[\bar{A}_1\right]\left[\bar{B}\right]\{V\} = \left[\bar{C}\right]\{V\}, \quad \left[\bar{C}\right] = \left[\bar{A}_1\right]\left[\bar{B}\right],\\
&\left\{V^{(4)}\right\} = \left[\bar{A}\right]\left\{V^{(3)}\right\} = \left[\bar{A}\right]\left[\bar{C}\right]\{V\} = \left[\bar{D}\right]\{V\}, \quad \left[\bar{D}\right] = \left[\bar{A}\right]\left[\bar{C}\right].
\end{aligned} \tag{29}$$

It should be noted that the above formulations are also employed for the transversal displacement W.

The discretized equations of motion are expressed in the following eigenvalue problem:

$$\left(-\lambda^2[M] + j\lambda[G] + K\right)\cdot(U,V,W)^T = 0, \tag{30}$$

where M, G, and K are the mass, gyroscopic and stiffness matrices, respectively. When $\Omega = 0$, the system is reduced to be undamped without gyroscopic effect, i.e.,

$$\left(-\lambda^2[M] + K\right)\cdot(U,V,W)^T = 0. \tag{31}$$

In order to solve the general eigenvalue problem, equation (30) is transformed to be

$$-\lambda^2\left[\hat{A}\right]\dot{u}_{tr} + \left[\hat{B}\right]u_{tr} = 0, \tag{32}$$

where

$$\left[\hat{A}\right] = \begin{bmatrix}[M] & 0\\ 0 & [K]\end{bmatrix}, \quad \left[\hat{B}\right] = \begin{bmatrix}[G] & [K]\\ -[K] & O\end{bmatrix}, \quad \dot{u}_{tr} = \begin{bmatrix}\dot{u}\\ u\end{bmatrix}. \tag{33}$$

A MATLAB code was developed to address the complex eigenvalue problem formulated from the two coupled flexural equations expressed in terms of the displacement components V and W. The results obtained from this numerical implementation are then analyzed to examine the effects of small-scale parameters, angular velocity, and boundary conditions on the vibration behavior of the system.

5. Selected results and discussions

5.1. Convergence study and validation

In the aim of confirming the efficiency and accuracy of the presented numerical procedure, Table 1 shows the convergence study of the first six frequency parameters λ, i.e.,

$$\lambda = \sqrt{\frac{\varrho A L^4 \omega^2}{EI}} \tag{34}$$

for the S-S nanobeam. It is clearly observed that the frequency parameters converge with the increasing of the number of grid points N and become stable at sixteen grid points that are sufficient to obtain converged results for the upcoming results. A single-walled carbon nanotube (SWCNT) of the following parameters was used: $L = 10d$, $d = 0.678\,\text{nm}$, $E = 5.5\,\text{TPa}$, $I = 4/64\pi d$.

Our results have been validated by comparing the flexural frequency parameters with those presented by Chakraverty and Behera [8] for different boundary conditions (simply supported beam, simply supported-clamped beam and clamped-clamped beam). The obtained frequency parameters are found to be in good agreement for both the local and nonlocal beam [4] using the following parameters: length $L = 100d$, diameter $d = 1\,\text{nm}$ (where the solid nanoshaft is not hollow), Young modulus $E = 2.1\,\text{TPa}$, density $\varrho = 7800\,\text{kg m}^{-3}$, Poisson's ratio $\nu = 0.3h$, and hub-radius factor $h/d = 0.02$.

Table 1. First six frequency parameters λ

N	4	6	8	12	16	20	24
λ	3.13432	3.1416	3.1415	3.1415	3.1415	3.1415	3.1415
	6.9282	6.2859	6.2833	6.2831	6.2831	6.2831	6.2831
	8.8417	9.1288	9.4202	9.4247	9.4247	9.4247	9.4247
	154.358	16.0982	12.7319	12.5662	12.5663	12.5663	12.5663
	176.411	17.2856	14.8290	15.7027	15.7079	15.7079	15.7079
	198.456	154.3598	28.3974	18.9325	18.8496	18.8495	18.8495

5.2. Effect of physical properties on the fundamental frequency parameters

Fig. 2 shows the Campbell diagram presenting the fundamental frequency parameters with respect to the angular velocity parameters (ranging from 1 to 5) for a rotating nanoshaft having a full solid cross-section without considering the nonlocal parameter, considering S-S, C-C and S-C beam boundary conditions, respectively. The figure shows that the frequency parameter is divided into two frequency values having a linear relationship with the angular velocities. The increasing frequency parameter is the forward frequency λ_f, whereas the decreasing one is the backward frequency λ_b. It is also remarked that the C-C frequency parameters are higher than those of S-C and S-S boundary conditions. The Campbell diagram serves to determine the critical speed where the nanoshaft vibrates violently, it is the angular velocity parameter correspondent to the intersection of the frequency parameter curves and the angular velocity parameters curves. Generally, the backward frequency should be of major interest in security applications and health monitoring of rotating machinery.

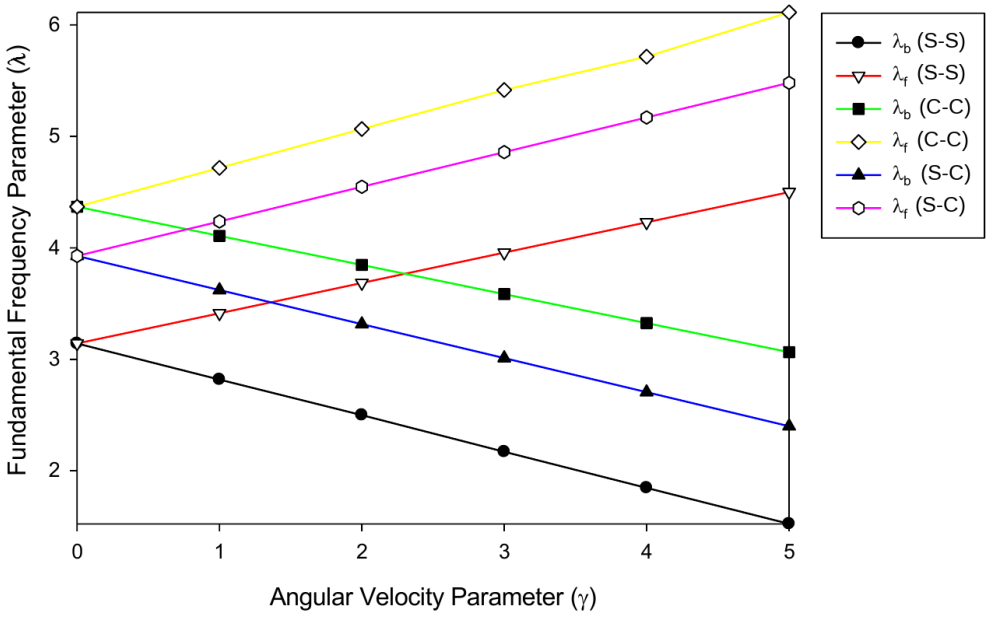

Fig. 2. Campbell diagram for different boundary conditions and $\mu^2 = 0$

At the nanoscale, the selection of the nonlocal parameter $(e_0\, a)^2$ is not arbitrary and must be physically justified. Our approach to this issue is twofold, addressing both the choice of the parameter range and the inherent size-dependency captured by the nonlocal theory itself. $(e_0 a)^2$ is chosen to range from 0 to 0.5 as a standard and practical range used extensively in the literature to model nanostructures of lengths between 2–20 nm, ensuring our results are consistent with established physical observations and theoretical benchmarks.

In Table 2, we have reported the bending forward and backward frequency parameters with respect to the angular velocity parameters for different scaling effect parameters (having the values of 0.1, 0.3, and 0.5). Results show the effect of the scaling parameters on the bending frequency parameters that decrease with increasing nonlocal parameters for all types of boundary conditions. It is observed that an increasing variation of 0.1 of nonlocal parameter can decrease the frequency parameter with an average percentage of 4 % for S-S, 2.5 % for C-C and 3 % for S-C boundary conditions.

Fig. 3 shows the fundamental critical speed with respect to the nonlocal parameter for different boundary conditions by increasing the nonlocal parameter, a logical decreasing is remarked in the critical speed parameters that are corresponding to values at $\lambda = \gamma$. For the local nano-rotor, the critical first speed is: 2.3992, 3.4803, and 3.0414 for S-S, C-C, and S-C boundary conditions, respectively. It is observed that the decreasing value of the critical speed is different for each type of boundary conditions.

5.3. Effect of geometrical properties on the fundamental mode frequency parameters

In order to investigate the effect of geometrical properties on the vibrational behavior of the nano-rotor, a parametric study has been done, taking into consideration the aspect ratio L/d and the ratio h/d. Figs. 4, 5, and 6 illustrate the variation of the first critical speed as a function of the aspect ratio L/d defined as a non-dimensional value by $1/\sigma$ for S-S, C-C, and S-C boundary conditions, respectively. The figures show that if the aspect ratio increases, the critical speed parameter decreases until the value of $1/\sigma = 100$, where the decreasing curve of the critical

Table 2. Fundamental frequency parameters of the rotating nanoshaft for different angular velocity parameters and nonlocal parameters (solid nanoshaft not hollow)

BCs	γ	$\mu^2 = 0.1$		$\mu^2 = 0.3$		$\mu^2 = 0.5$	
		λ_b	λ_f	λ_b	λ_f	λ_b	λ_f
S-S	0	3.0111	3.0111	2.6800	2.6800	2.3022	2.3022
	1	2.6873	3.5439	2.3940	2.9860	2.0258	2.6118
	2	2.3687	3.8156	2.1440	3.2920	1.7494	2.9214
	3	2.0400	4.0873	1.8220	3.5980	1.4730	3.2310
	4	1.7167	4.3590	1.5360	3.9040	1.1966	3.5406
	5	1.3927	4.6307	1.2500	4.2100	0.9202	3.8502
C-C	0	4.2587	4.3587	3.9100	3.9100	3.3155	3.3155
	1	3.9977	4.2177	3.6780	4.2780	3.0766	3.7004
	2	3.8367	5.1765	3.4460	4.6460	2.8377	4.0853
	3	3.4757	5.5256	3.2140	5.0140	2.5988	4.4702
	4	3.2147	5.8243	2.9820	5.3820	2.3599	4.8551
	5	2.9537	6.2232	2.7500	5.7500	2.1200	5.2400
S-C	0	3.8036	3.8036	3.2828	3.2828	2.7899	2.7899
	1	3.4983	4.3603	3.0022	3.6062	2.5219	3.1301
	2	3.1930	4.6710	2.7216	3.9296	2.2539	3.4703
	3	2.8877	4.9817	2.4410	4.2530	1.9859	3.8105
	4	2.5824	5.2924	2.1604	4.5764	1.7179	4.1507
	5	2.2771	5.6031	1.8789	4.9000	1.4500	4.4910

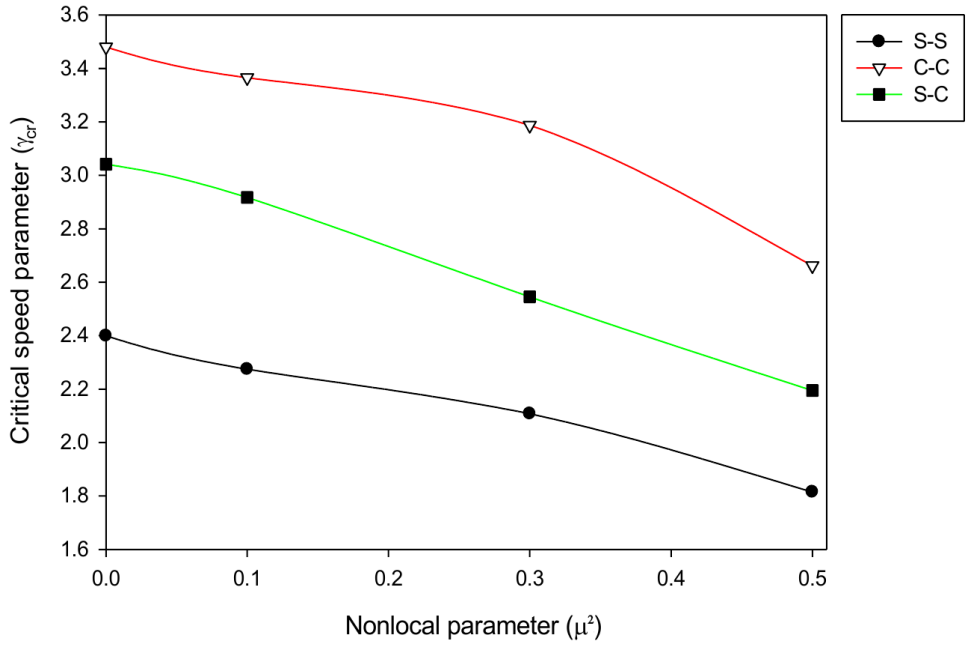

Fig. 3. First critical speed parameter for different nonlocal parameters and boundary conditions

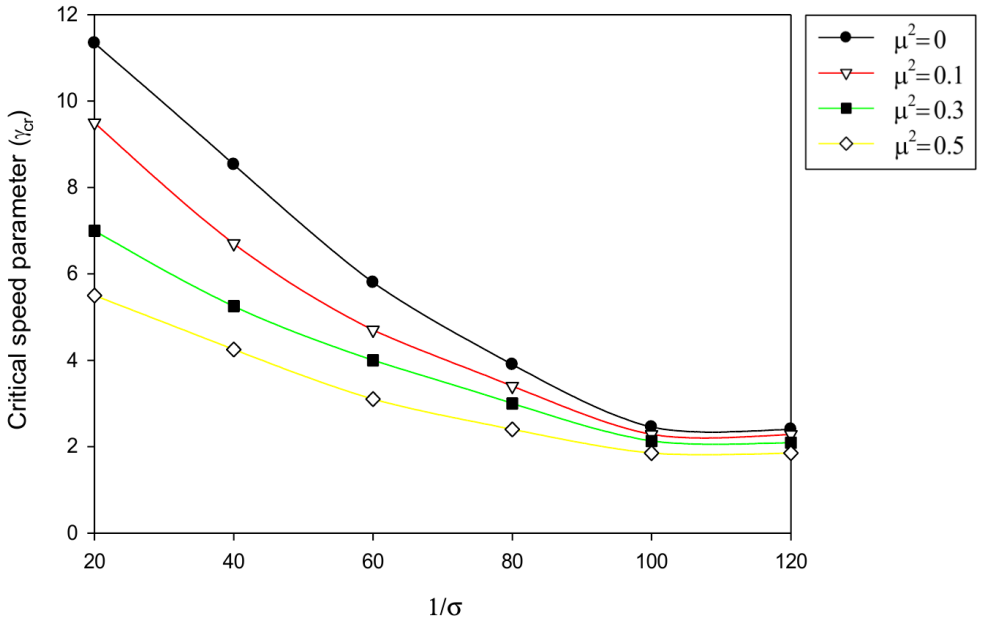

Fig. 4. First critical speed parameter against $1/\sigma$ for different nonlocal parameters and S-S boundary conditions

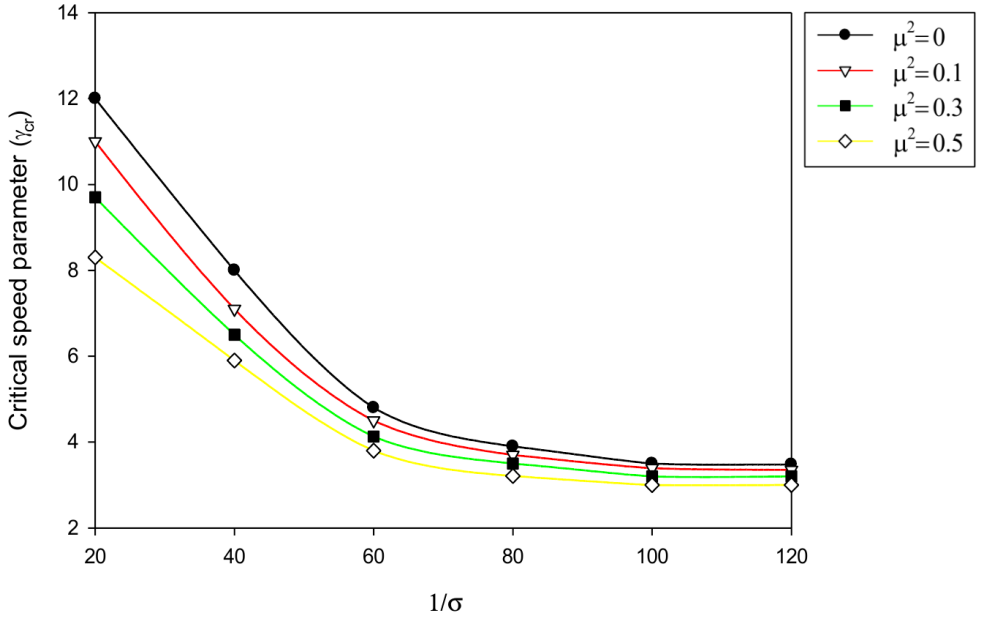

Fig. 5. First critical speed parameter against $1/\sigma$ for different nonlocal parameters and C-C boundary conditions

speed becomes straight and stable. The nonlocal parameter decreases the critical speed parameters when it increases for all boundary conditions. It is observed that the shape of the critical speed curves are qualitatively similar.

The effect of hub-radius on the variation of critical speed parameters is investigated for different boundary conditions. Figs. 7, 8, and 9 give the critical speed parameters with respect to thickness-diameter ratio of the nano-rotor. It is clearly remarkable that the influence of the thickness for a constant length is neglected for all boundary conditions. The curves are identical in shape and different in value due to the type of boundary conditions. The effect of the nonlocal

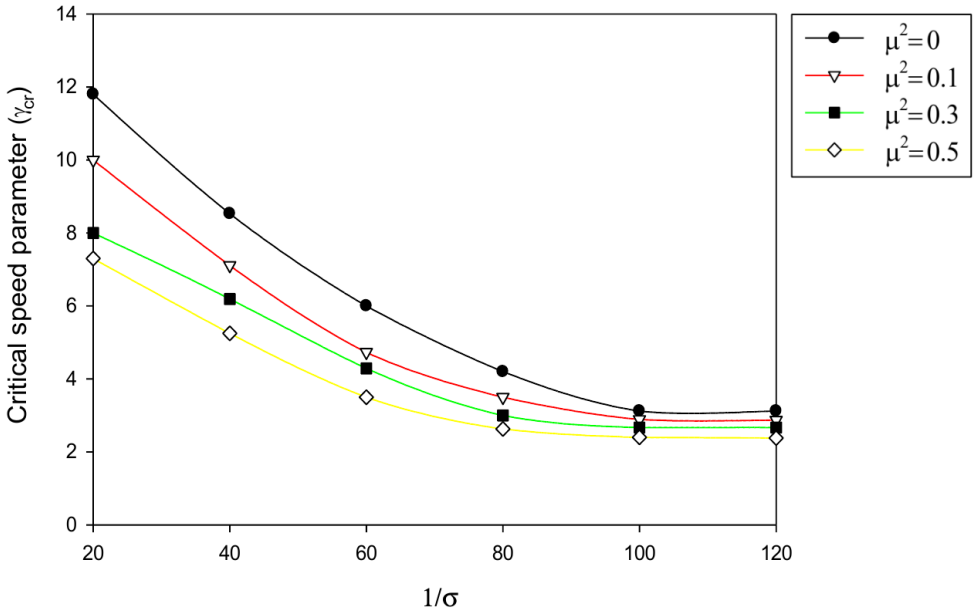

Fig. 6. First critical speed parameter against $1/\sigma$ for different nonlocal parameters and S-C boundary conditions

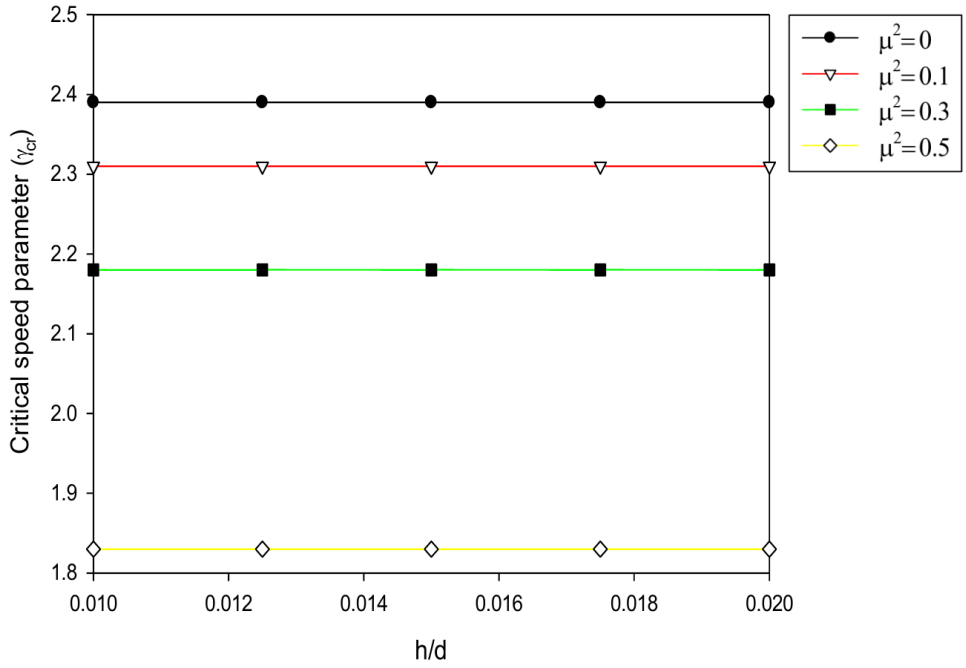

Fig. 7. First critical speed parameter against h/d for different nonlocal parameters and S-S boundary conditions

parameter stays significant.

5.4. Effect of physical properties on the second mode frequency parameters

In this section, the second mode frequency parameters are analyzed. Table 3 shows that an increase in the small-scale parameter decreases the frequency parameters of the second mode. In comparison with those of the first mode, the decrease in frequency parameters is smaller for the second mode than in the fundamental mode. The same effects of the angular velocity

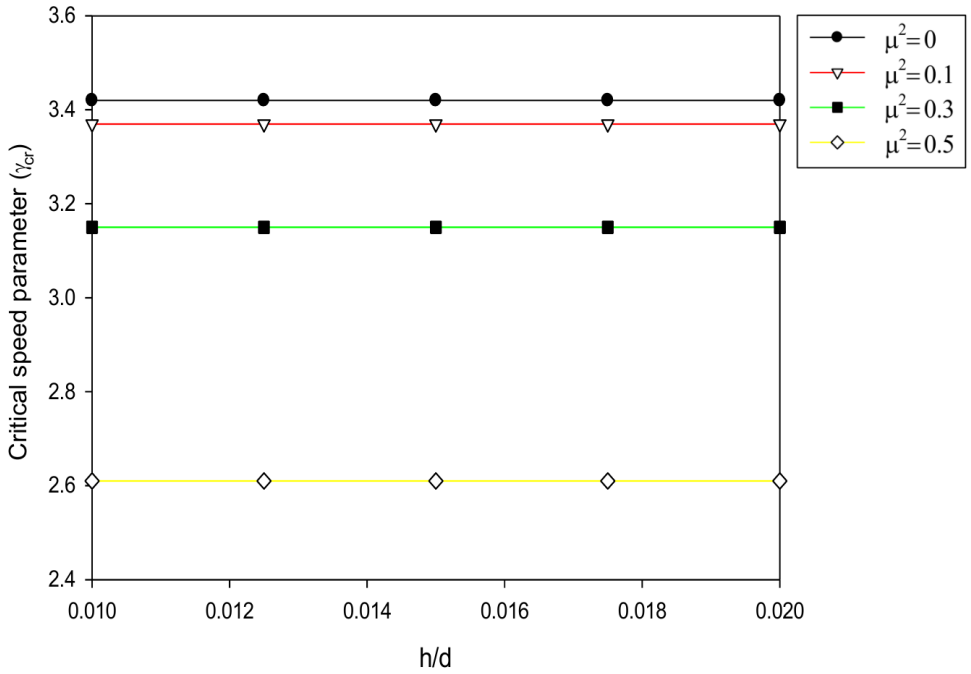

Fig. 8. First critical speed parameter against h/d for different nonlocal parameters and C-C boundary conditions

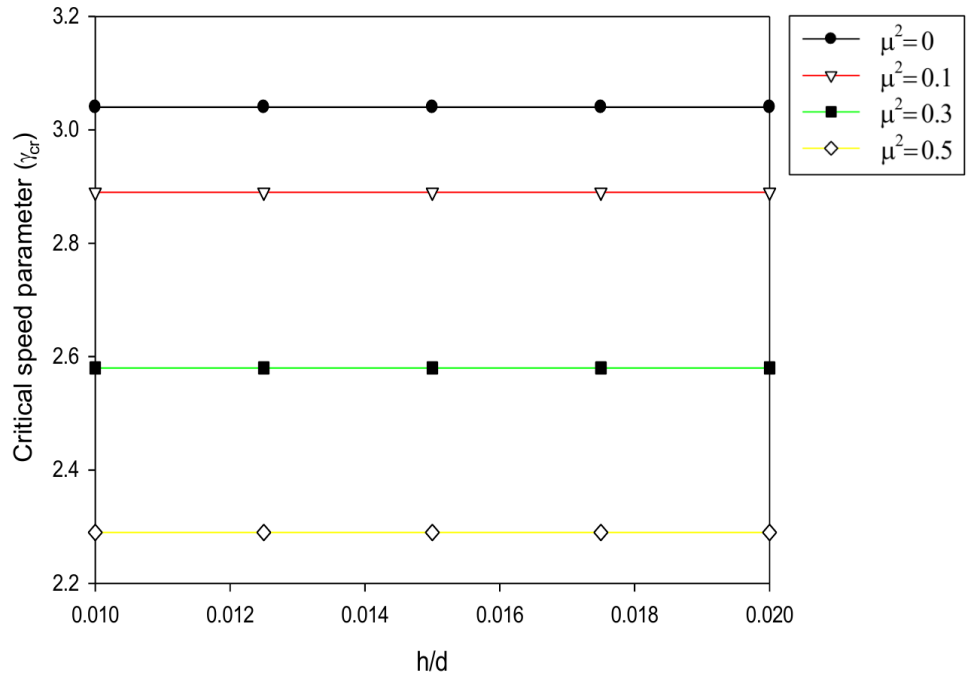

Fig. 9. First critical speed parameter against h/d for different nonlocal parameters and S-C boundary conditions

parameter and the boundary conditions on the fundamental frequency parameters remain valid for the second mode.

Fig. 10 shows the Campbell diagram for the second mode frequency parameters that are divided to forward and backward frequency parameters. It is also remarkable that the curves for different nonlocal parameters are close to each other. This shows that the nonlocal parameter has a small effect on the second mode frequency parameter than the fundamental ones. Fig. 11

Table 3. Second mode frequency parameters of the rotating nanoshaft for different μ^2

BCs	γ	$\mu^2 = 0.1$		$\mu^2 = 0.3$		$\mu^2 = 0.5$	
		λ_b	λ_f	λ_b	λ_f	λ_b	λ_f
SS	0	6.1236	6.1236	6.0006	6.0006	5.9136	5.9024
	1	5.6854	6.8503	5.5624	6.7273	5.4754	6.6291
	2	5.2733	7.1622	5.1503	7.0392	5.0633	6.941
	3	4.9501	7.6631	4.8271	7.5401	4.7401	7.4419
	4	4.5394	8.0154	4.4164	7.8924	4.3294	7.7942
	5	4.1643	8.4022	4.0413	8.2792	3.9543	8.181
	6	3.7883	8.7022	3.6653	8.5792	3.5783	8.481
C-C	0	7.7788	7.7788	7.6114	7.6114	7.5244	7.5244
	1	7.3791	8.3397	7.2117	8.1641	7.1247	6.9573
	2	7.0122	8.7395	6.8448	8.5639	6.7578	6.5904
	3	6.6325	9.0608	6.4651	8.8852	6.3781	6.2107
	4	6.2924	9.4559	6.125	9.2803	6.038	5.8706
	5	5.9098	9.8048	5.7424	9.6292	5.6554	5.488
	6	5.6104	10.126	5.443	9.9509	5.356	5.1886
S-C	0	7.0686	7.0686	7.0686	7.0686	7.0686	7.0686
	1	6.545	7.5782	6.534	7.5902	6.516	7.6072
	2	6.1629	7.931	6.1519	7.943	6.1339	7.9652
	3	5.8101	8.341	5.7991	8.353	5.7811	8.3711
	4	5.5165	8.6663	5.5055	8.6783	5.4875	8.6953
	5	5.1146	9.0226	5.1036	9.0346	5.0856	9.0516
	6	4.7295	9.3607	4.7185	9.3727	4.7005	9.3897

shows the critical speed parameters of the second mode, which are decreasing with the increase of the small-scale effect.

6. Summary and concluding remarks

This study successfully investigated the linear free vibration characteristics of a nano-rotor by employing the Eringen's nonlocal elasticity theory to capture size-dependent effects. The governing equations, derived via Hamilton's principle, were solved using a novel MATLAB code developed to handle the complex eigenvalue problem inherent to systems with gyroscopic effects. The generalized differential quadrature method (GDQM) proved to be an effective numerical approach for this nanoscale dynamics problem, with results successfully validated against the existing literature.

The performed analysis provided several key insights into the parameters governing nano-rotor dynamics:

- *Rotational dynamics:* The gyroscopic effect inherently splits the frequency parameter into distinct forward and backward whirl modes. An increase in the critical speed parameter raises the forward frequency while suppressing the backward one.
- *Size-dependence:* The nonlocal parameter exerts a significant influence, with its increase

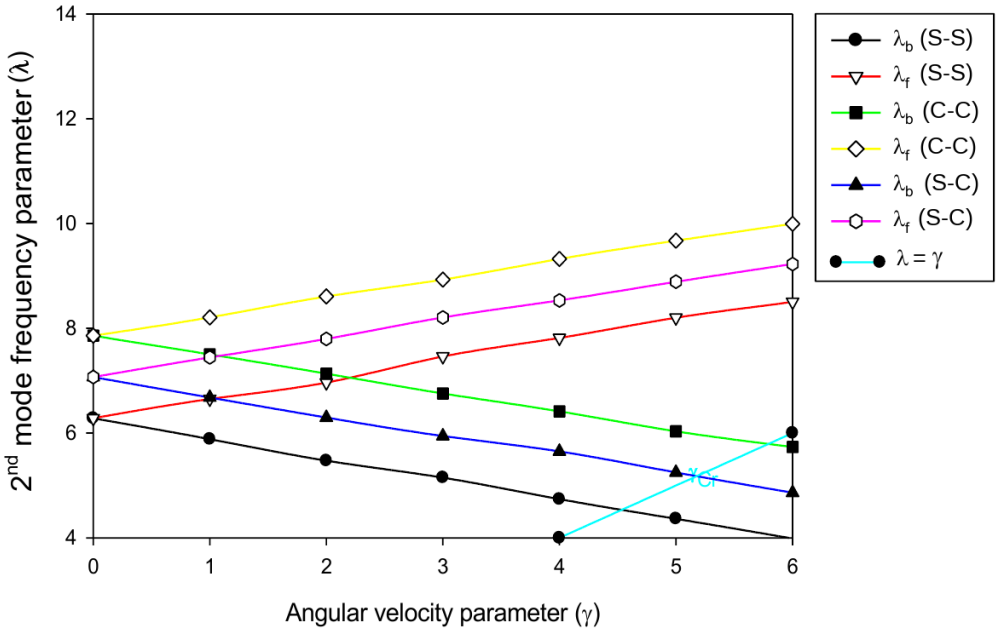

Fig. 10. Campbell diagram of the 2nd mode frequency parameter for different boundary conditions and $\mu^2 = 0.3$

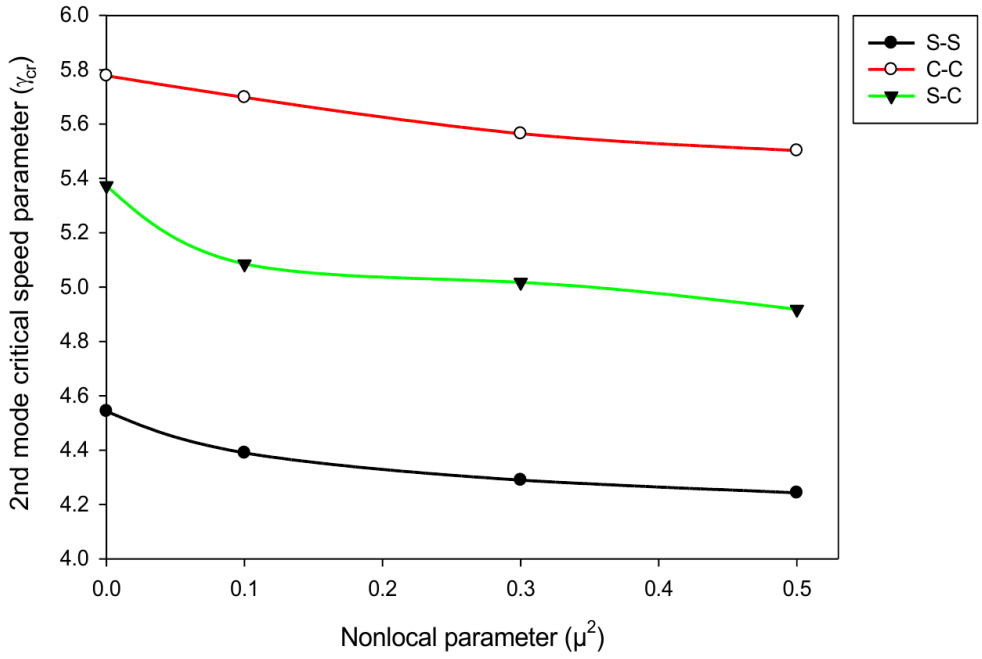

Fig. 11. Critical speed of the 2nd mode frequency parameter for different boundary conditions and μ^2

leading to a softening effect that reduces both the frequency and critical speed parameters across all boundary conditions. This quantitatively demonstrates the crucial role of size-dependent material behavior in nanostructure dynamics.

- *Geometric and boundary effects:* Among the boundary conditions studied, clamped-clamped (C-C) boundary condition yielded the highest frequency parameters. While the aspect ratio negatively impacts the critical speed, its influence diminishes at higher values. Notably, the hub-radius was found to have a negligible effect on the dynamic response.

Our study explicitly and quantitatively accounts for the size-dependent material behavior that is intrinsic to nanostructures. The results demonstrate how the dynamic characteristics (frequencies, critical speeds) of the rotating nanoshaft are not fixed but vary significantly with the size of the structure, as governed by the nonlocal parameter. This provides the practical, size-specific design insight that is crucial for NEMS applications.

The results of this report can serve as a guidance in the design of rotating nano-machinery, such as nano-turbines, nano-motors, nano-rotors, nano-blades and other nano-rotational devices involved in medicine and biology.

Acknowledgement

This work was supported in part by the Laboratory of Computational Mechanics (MECA-COMP), Department of Mechanical Engineering, Faculty of Technology, University of Tlemcen, Algeria under reference (PRFU: A11N01UN130120180001).

References

[1] Arash, B., Wang, Q., A review on the application of nonlocal elastic models in modeling of carbon nanotubes and graphenes, Computational Material Science 51 (1) (2012) 303–313. https://doi.org/10.1016/j.commatsci.2011.07.040

[2] Barooti, M. M., Safarpour, M., Ghadiri, H., Critical speed and free vibration analysis of spinning 3D single-walled carbon nanotubes resting on elastic foundations, The European Physical Journal Plus 132 (2017) No. 6. https://doi.org/10.1140/epjp/i2017-11275-5

[3] Bellman, R. Kashef, B. G., Casti, J., Differential quadrature: A technique for the rapid solution of nonlinear partial differential equations, Journal of Computational Physics 10 (1) (1972) 40–52. https://doi.org/10.1016/0021-9991(72)90089-7

[4] Belhadj, A., Boukhalfa, A., Belalia, S. A., Free vibration analysis of a rotating nanoshaft based SWCNT, European Physical Journal Plus 132 (2017) No. 513. https://doi.org/10.1140/epjp/i2017-11783-2

[5] Bert, C. W., Malik, M., Differential quadrature method in computational mechanics: A review, Applied Mechanics Review 49 (1) (1996) 1–28. https://doi.org/10.1115/1.3101882

[6] Bishop, R. E. D., The vibration of rotating shafts, Journal of Mechanical Engineering Science 1 (1) (1959) 50–65. https://doi.org/10.1243/JMES_JOUR_1959_001_009_02

[7] Bourlon, B., Glattli, D. C., Miko, C., Forró, L., Bachtold, A., Carbon nanotube based bearing for rotational motions, Nano Letters 4 (4) (2004) 709–712. https://doi.org/10.1021/nl035217g

[8] Chakraverty, S., Behera, L., Free vibration of non-uniform nanobeams using Rayleigh-Ritz method, Physica E: Low-dimensional Systems and Nanostructures 67 (2015) 38–46. https://doi.org/10.1016/j.physe.2014.10.039

[9] Chong, K. P., Nano science and engineering in solid mechanics, Acta Mechanica Solida Sinica 21 (2008) 95–103. https://doi.org/10.1007/s10338-008-0812-7

[10] de Sciarra, F. M., Barretta, R., A new nonlocal bending model for Euler-Bernoulli nanobeams, Mechanics Research Communications 62 (2014) 25–30. https://doi.org/10.1016/j.mechrescom.2014.08.004

[11] Drexler, K. E., Nanosystems: Molecular machinery, manufacturing, and computation, Wiley, New York, 1992.

[12] Du, H., Lim, M. K., Lin, R. M., Application of generalized differential quadrature method to structural problems, International Journal of Numerical Methods in Engineering 37 (11) (1994) 1 881–1 896. https://doi.org/10.1002/nme.1620371107

[13] Dutt, J. K., Nakra, B. C., Dynamics of rotor shaft system on flexible supports with gyroscopic effects, Mechanics Research Communications 22 (6) (1995) 541–545. https://doi.org/10.1016/0093-6413(95)00059-3

[14] Ebrahimi, F., Hashemi, M., On vibration behavior of rotating functionally graded double-tapered beam with the effect of porosities, Proceedings of the Institution of Mechanical Engineers, Part G: Journal of Aerospace Engineering 230 (10) (2016) 1 903–1 916. https://doi.org/10.1177/0954410015619647

[15] Eringen, A. C., Nonlocal polar elastic continua, International Journal of Engineering Science 10 (1) (1972) 1–16. https://doi.org/10.1016/0020-7225(72)90070-5

[16] Eringen, A. C., On differential equations of nonlocal elasticity and solutions of screw dislocation and surface waves, Journal of Applied Physics 54 (9) (1983) 4 703–4 710. https://doi.org/10.1063/1.332803

[17] Eringen, A. C., Kim, B. S., Relation between nonlocal elasticity and lattice dynamics, Crystal Lattice Defects 7 (2) (1977) 51–57.

[18] Eltaher, M. A., Elshorbagy, A. E., Mahmoud, F. F., Vibration analysis of Euler-Bernoulli nano-beams by using finite element method, Applied Mathematical Modelling 37 (7) (2013) 4 787–4 797. https://doi.org/10.1016/j.apm.2012.10.016

[19] Ekinci, K. L., Roukes, M. L., Nanoelectromechanical systems, Review of Scientific Instruments 76 (6) (2005) No. 061101. https://doi.org/10.1063/1.1927327

[20] Fennimore, A. M., Yuzvinsky, T. D., Han, W. Q., Fuhrer, M. S., Cumings, J., Zettl, A., Rotational actuators based on carbon nanotubes, Nature 42 (2003) 408–410. https://doi.org/10.1038/nature01823

[21] Fernández-Sáez, J., Zaera, R., Loya, J. A., Reddy, J. N., Bending of Euler-Bernoulli beams using Eringen's integral formulation: A paradox resolved, International Journal of Engineering Science 99 (2016) 107–116. https://doi.org/10.1016/j.ijengsci.2015.10.013

[22] Foroutan, M., Fatemi, S. M., Molecular dynamics simulations of systems containing nanostructures, In: Encyclopedia of Nanoscience and Nanotechnology, (editor) H. S. Nalwa, American Scientific Publishers, 2016, pp. 1–29.

[23] Friswell, M. I., Penny, J. E. T., Garvey, S. D., Lees, A. W., Dynamics of rotating machines, Cambridge Aerospace Series, 2010. https://doi.org/10.1017/CBO9780511780509

[24] Gartia, A. K. Chakraverty, S., Advanced computational modeling and mechanical behavior analysis of multi-directional functionally graded nanostructures: A comprehensive review, Computer Modelling in Engineering Science 142 (3) (2025) 2 405–2 455. https://doi.org/10.32604/cmes.2025.061039

[25] Gartia, A. K., Priya, R., Chakraverty, S., Analytical solution for free vibration of multi-cracked metal-ceramic functionally graded nanobeams resting on elastic foundations, International Journal of Structural Stability and Dynamics (2025). https://doi.org/10.1142/S0219455426504006

[26] Ghadiri, M., Shafiei, N., Nonlinear bending vibration of a rotating nanobeam based on nonlocal Eringen's theory using differential quadrature method, Microsystem Technology 22 (2016) 2 853–2 867. https://doi.org/10.1007/s00542-015-2662-9

[27] Guskov, M., Sinou, J.-J., Thouverez, F., Multi-dimensional harmonic balance applied to rotor dynamics, Mechanics Research Communications 35 (8) (2008) 537–545. https://doi.org/10.1016/j.mechrescom.2008.05.002

[28] Iijima, S., Helical microtubules of graphitic carbon, Nature 354 (1991) 56–58. https://doi.org/10.1038/354056a0

[29] Jena, S. K., Chakraverty, S., Free vibration analysis of single walled carbon nanotube with exponentially varying stiffness, Curved and Layered Structures 5 (1) (2018) 201–212. https://doi.org/10.1515/cls-2018-0015

[30] Johnson, D. C., Free vibration of a rotating elastic body: The general theory and some examples of practical cases, Aircraft Engineering and Aerospace Technology 24 (8) (1952) 234–236. https://doi.org/10.1108/eb032192

[31] Lo, D. C., Young, D. L., Tsai, C. C., High resolution of 2D natural convection in a cavity by the DQ method, Journal of Computational and Applied Mathematics 203 (1) (2007) 219–236. https://doi.org/10.1016/j.cam.2006.03.021

[32] Marzani, A., Tornabene, F., Viola, E., Nonconservative stability problems via generalized differential quadrature method, Journal of Sound and Vibration 315 (1–2) (2008) 176–196. https://doi.org/10.1016/j.jsv.2008.01.056

[33] Hosseini-Hashemi, S., Ilkhani, M. R., Fadaee, M., Accurate natural frequencies and critical speeds of a rotating functionally graded moderately thick cylindrical shell, International Journal of Mechanical Science 76 (2013) 9–20. https://doi.org/10.1016/j.ijmecsci.2013.08.005

[34] Murmua, T., Adhikari, S., Scale-dependent vibration analysis of prestressed carbon nanotubes undergoing rotation, Journal of Applied Physics 108 (12) (2010) No. 123507. https://doi.org/10.1063/1.3520404

[35] Narendar, S., Differential quadrature based nonlocal flapwise bending vibration analysis of rotating nanotube with consideration of transverse shear deformation and rotary inertia, Applied Mathematics and Computation 219 (3) (2012) 1 232–1 243. https://doi.org/10.1016/j.amc.2012.07.032

[36] Nejad, M. Z., Hadi, A., Eringen's nonlocal elasticity theory for bending analysis of bi-directional functionally graded Euler-Bernoulli nano-beams, International Journal of Engineering Science 106 (2025) 1–9. https://doi.org/10.1016/j.ijengsci.2016.05.005

[37] Torkaman-Asadi, M. A., Rahmanian, M., Firouz-Abadi, R. D., Free vibrations and stability of high-speed rotating carbon nanotubes partially resting on Winkler foundations, Composite Structure 126 (2015) 52–61. https://doi.org/10.1016/j.compstruct.2015.02.037

[38] Pisano, A. A., Fuschi, P., Polizzotto, C., Integral and differential approaches to Eringen's nonlocal elasticity models accounting for boundary effects with applications to beams in bending, Journal of Applied Mathematics and Mechanics – Zeitschrift für Angewandte Mathematik und Mechanik 101 (8) (2021) No. e202000152. https://doi.org/10.1002/zamm.202000152

[39] Pradhan, S. C., Murmu, T., Application of nonlocal elasticity and DQM in the flapwise bending vibration of a rotating nanocantilever, Physica E: Low-dimensional Systems and Nanostructures 42 (7) (2010) 1 944–1 949. https://doi.org/10.1016/j.physe.2010.03.004

[40] Reddy, J. N., Nonlocal theories for bending, buckling and vibration of beams, International Journal of Engineering Science 45 (2–8) (2007) 288–307. https://doi.org/10.1016/j.ijengsci.2007.04.004

[41] Reddy, J. N., Energy principles and variational methods in applied mechanics, John Wiley & Sons Inc., 2002.

[42] Sae-Long, W., Limkatanyu, S., Rungamornrat, J., Prachasaree, W., Sukontasukkul, P., Sedighi, H. M., A rational beam-elastic substrate model with incorporation of beam-bulk nonlocality and surface-free energy, The European Physical Journal Plus 136 (2021) No. 80. https://doi.org/10.1140/epjp/s13360-020-00992-7

[43] Sae-Long, W., Limkatanyu, S., Sukontasukkul, P., Damrongwiriyanupap, N., Rungamornrat, J., Prachasaree, P., Fourth-order strain gradient bar-substrate model with nonlocal and surface effects for the analysis of nanowires embedded in substrate media, Facta Universitatis 19 (4) (2025) 657–680. https://doi.org/10.22190/FUME201009045S

[44] Shaat, M., A general nonlocal theory and its approximations for slowly varying acoustic waves, International Journal of Mechanical Sciences 130 (2017) 52–63. https://doi.org/10.1016/j.ijmecsci.2017.05.038

[45] Shi, J., Wang, Z., Chen, Z., Concurrence of oscillatory and rotation of the rotors in a thermal nanotube motor, Computational Material Science 120 (2016) 94–98. https://doi.org/10.1016/j.commatsci.2016.04.005

[46] Shi, J., Liu, L. N., Cai, K., Qin, Q.-H., Conditions for escape of a rotor in a rotary nanobearing from short triple-wall nanotubes, Scientific Reports 7 (2017) No. 6772. https://doi.org/10.1038/s41598-017-07184-x

[47] Shafiei, N., Kazemi, M., Ghadiri, M., Nonlinear vibration behavior of a rotating nanobeam under thermal stress using Eringen's nonlocal elasticity and DQM, Applied Physics A 122 (2016) No. 728. https://doi.org/10.1007/s00339-016-0245-y

[48] Shu, C., Richards, B. E., Application of generalized differential quadrature to solve two-dimensional incompressible Navier-Stokes equations, International Journal for Numerical Methods in Fluids 15 (7) (1992) 791–798. https://doi.org/10.1002/fld.1650150704

[49] Tufekci, E., Aya, S. A., A nonlocal beam model for out-of-plane static analysis of circular nanobeams, Mechanics Research Communications 76 (2016) 11–23. https://doi.org/10.1016/j.mechrescom.2016.06.002

[50] Timoshenko, S., Young, D. H., Advanced dynamics, McGraw-Hill Book Company, Inc., 1948.

[51] Tornabene, F., Fantuzzi, N., Bacciocchi, M., The local GDQ method applied to general higher-order theories of doubly curved laminated composite shells and panels: The free vibration analysis, Composite Structures 116 (2014) 637–660. https://doi.org/10.1016/j.compstruct.2014.05.008

[52] Thai, H.-T., A nonlocal beam theory for bending, buckling, and vibration of nanobeams, International Journal of Engineering Science 52 (2012) 56–64. https://doi.org/10.1016/j.ijengsci.2011.11.011